6th International Conference on NDE in Relation to Structural Integrity for Nuclear and Pressurized Components
October 2007, Budapest, Hungary
For more papers of this publication click: www.ndt.net/search/docs.php3?MainSource=70

Developments in Ultrasonic Inspection II

SAFT Performance in Ultrasonic Inspection of Coarse Grained Metals

T. Stepinski, Uppsala University- Signals and Systems, Sweden

ABSTRACT

Experience from the ultrasonic inspection of nuclear power plants has shown that large focused transducers are relatively effective in suppressing material structure noise. Operation of a large focused transducer can be thought of as integration (coherent summation) of individual beams reflected from the flaw and received by individual points at the transducer surface.

Synthetic aperture focusing technique (SAFT), in its simplest version mimics an acoustic lens used for focusing ultrasonic beams at a desired point in the region of interest. Thus, SAFT should be able to suppress structure noise in the similar way as focused transducer does.

This paper presents the results of investigation of SAFT algorithms applied for post-processing of ultrasonic data acquired in inspection of coarse grained metal specimens. The performance of SAFT in terms of its spatial resolution and grain noise suppression is studied. The evaluation is made based on the experimental data obtained from the ultrasonic inspection of test specimens with artificial defects (side drilled holes). SAFT algorithms for both contact and immersion mode are reviewed and experimentally verified.

INTRODUCTION

Ultrasonic images show a characteristic granular structure commonly known as speckle in medical applications and grain (structure) noise in NDE. Speckle in ultrasonic images arises from the presence of tiny scatterers in the range cell. The speckle, which is a common artifact of diffraction limited imaging, reduces the detection capability of ultrasonic imaging systems and indirectly affects the identification of specific reflectors in the regions of interest (ROI).

Speckle can be reduced through diversity techniques that involve averaging the multiple images created either through frequency compounding or spatial compounding.

Frequency compounding involves decomposition of an image obtained with a broadband transducer into a number of narrowband images and detecting correlations between those images. Split spectrum processing (SSP) is a well known technique belonging to this class.

In spatial compounding, the multiple images are produced by viewing the ROI from various spatial locations, angles or orientations of a transducer. Spatial compounding reduces speckle and increases image contrast by incoherently averaging different images of the same ROI. The term incoherent means that the envelope of the RF A-scans is calculated first, and then a brightness B-scan is obtained by aggregating those A-scans (this is a standard way of presenting results in medical applications).

Coherent averaging of RF images is generally difficult in medical applications due to tissue movements and inaccurately known transducer position. However, the situation in most NDE applications is different since the test object is stationary and transducer position can be measured very accurately.

Experience from the inspection of nuclear reactors has shown that large focused transducers are relatively effective in suppressing grain noise. Operation of a large focused transducer can be thought of as integration (coherent summation) of the individual beams reflected from the target and received by individual points at the transducer surface. The use of such transducers, however, is limited by practical reasons – they are bulky and inflexible (fixed focus).

Recently, advanced synthetic aperture (SA) algorithms characterized by an enhanced spatial resolution, especially in near field have been developed in our group [1-3]. SA algorithms are based on coherent summation of ultrasonic signals received by a transducer in different locations. In the simplest version, the SA algorithm mimics a physical lens in focusing beams in a desired point of

ROI. The advantage, however, is that by a suitable post-processing of the received A-scans SA can produce the focusing effect in all points of ROI simultaneously.

The main aim of this paper is to investigate performance of SA used for the inspection of grainy materials in terms of resolution and grain noise suppression. We apply SAFT algorithms to signals (B-scans) acquired from the test blocks characterized by large grains. The blocks have a number of representative artificial defects that are difficult to detect using standard means. The inspection is performed in contact and in immersion using standard ultrasonic transducers.

TIME-DOMAIN SAFT

In SAFT the pulse-echo measurements made at a multitude of transmitter/receiver locations are combined to form a map of the ultrasonic reflectivity of the insonified ROI. The method takes advantage of both spatial and temporal correlations to enhance the resolution and the signal-to-noise ratio of the resultant images. Time-domain SAFT (t-d SAFT) has been used in ultrasonic NDE mainly due to its two benefits: first, it is capable of improving lateral resolution in the focal zone, and second, it extends the focal zone resulting in a dynamic focusing effect, [4].

Most SAFT implementations in NDE are performed using a delay-and-sum (DAS) processing in time-domain [5, 6]. Usually, there is no prior knowledge about the defect positions in material, and the dynamic focusing in the ROI is performed to achieve the improved cross-range resolution. Different delays are applied in the DAS algorithm for different focal points in ROI to simulate the specific hyperbolas that correspond to the distances from the aperture to the particular focal point.

SAFT in Contact Mode

Let us illustrate the SAFT principle with a simple system model. Consider the measurement setup shown in Fig. 1, which is known in radar applications as a broadside strip-map mode synthetic aperture imaging system, [7]. This means that the SAFT system maintains its transducer beam at a broadside of the synthetic aperture throughout the data acquisition period.

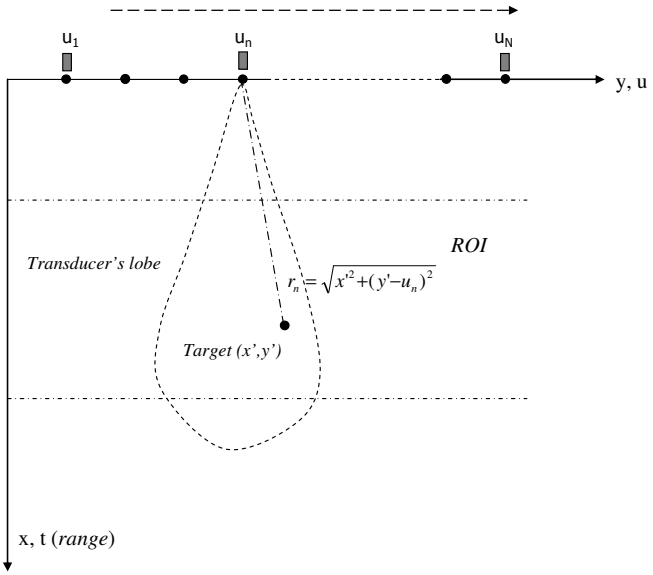

Figure 1 – 2D geometry appropriate for broadside strip-map mode synthetic aperture.

The ROI contains a number of reflecting targets (flaws) in the spatial (x,y) domain, where x denotes the range while y identifies the cross range. The transducer transmits a broad lobe and moves along the u axis, which is parallel to the y axis of the target area.

To achieve focus at an observation point (*x',y'*) in the ROI, the SAFT time-shifts and performs a summation of the received signals $e(t,u_n)$ measured at transducer positions u_n for all n in the synthetic aperture. Assuming that the point source element model is valid (that is the ROI is in the transducer's far-field), the DAS scheme of a t-d SAFT is illustrated by the block diagram shown in Fig. 2. The time delay, denoted by τ_n, which is used to compensate for pulse traveling time at the transducer position u_n will be

$$\tau_n = 2\left(\sqrt{R^2 + (u_n - y')^2} - R\right)$$

where y' is the y-coordinate of the target. Apodization coefficients a_n are used to control the side lobe levels.

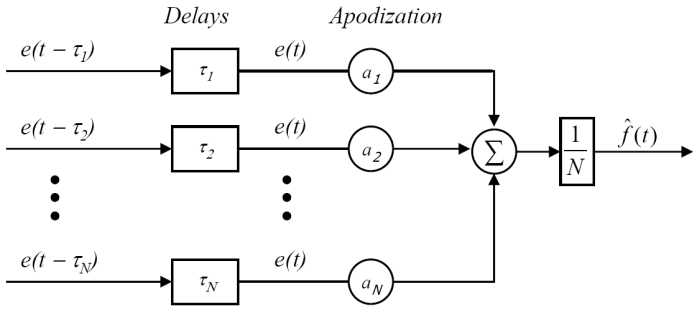

Figure 2 – Block diagram for the delay-and-sum SAFT system. DAS generates a sum of delayed signals received at different transducer positions. Each signal can also be multiplied by the apodization coefficient to reduce the side lobes in the resulting beampattern.

SAFT in Immersion Mode

For the immersion case, the acoustic path between the transducer and the target is no longer a straight line. The difference between water impedance and impedance of the inspected material, for instance, steel, results in the beam refraction at the object surface. According to the Fermat principle (expressed in the form of Snell law), the ultrasonic waves of a given length travel along the path between two points which takes the least time. The real path from the transducer position *A* to the target scatter *O* is indicated Fig. 3 by the solid line with arrows.

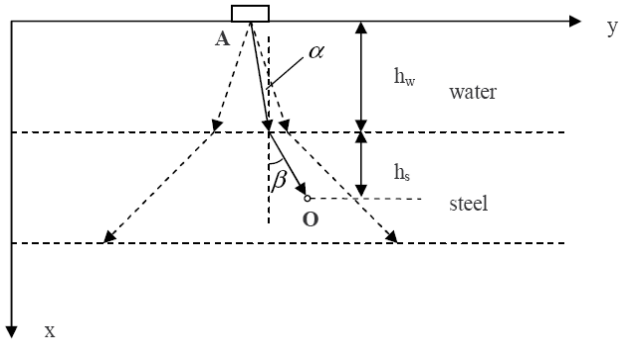

Figure 3 - Beam refraction in the immersion mode – the ultrasonic wave chooses the path between two points which takes the least time.

Let us denote the beam distance between the probe position u_n and the incident point by s_{wn} and the beam distance between the incidence point and the target in the object at (x',y') by s_{on}. Then the delay for the successive transducer positions is

$$\tau_n = 2\left(\frac{s_{wn}}{c_w} + \frac{s_{on}}{c_s}\right)$$

where c_w and c_s are acoustic speed in water and steel, respectively. To calculate the delays τ_n the values of s_{wn} and s_{on} have to be found first for each particular setup as a solution of a nonlinear equation resulting from the Fermat principle.

Effective Aperture Length

In order to determine the number of A-scans that should be included in the synthetic aperture we will introduce the concept of *effective aperture length*. The effective aperture length L_{eff} is motivated by the diffraction effects of the finite-sized transducer.

Generally, all transducers have some form of beam pattern that takes the form of a main lobe accompanied by a number of side lobes. The main lobe width is an important parameter that defines the transducer's cross-range resolution. The parameter L_{eff} is defined as the largest aperture length corresponding to wavelength λ that contributes to the SAFT performance in terms of its lateral resolution improvement. It is assumed that the signals received by all elements of a synthetic aperture are used efficiently if the L_{eff} is no longer than the half-power lobewidth of the transducer used in the aperture. For a circular transducer with diameter d the half-power lobewidth (the width between the -3dB points in the main lobe) at a distance R is (for details see [8, 3]). Thus for a certain transducer (for fixed d and λ), the longer the range, the longer is the L_{eff}. On the other hand, for a fixed range, smaller transducer diameter or lower transducer center frequency also results in longer L_{eff}.

Thus in the algorithms presented above, the L_{eff} depends on the target range and it should be recalculated for each range in the ROI.

Theoretical SAFT Performance

An important difference between the focusing the physical phased arrays and the SAFT is that the synthetic aperture has the cross-range resolution finer by a factor of 2 for the same number of elements that transmit and receives signals. Consequently, the SAFT -3dB cross range resolution is [8]

$$\delta_{3dB} \cong \frac{R\lambda}{2L_{eff}}$$

where L_{eff} is the effective synthetic aperture length, defined as the largest aperture length corresponding to the ultrasonic frequency that contributes to the SAFT performance in terms of its lateral resolution, and R is the focusing range.

Note that the above equation illustrates the fact that the synthetic aperture simulates a large physical aperture transducer using only one small element.

If the expression for L_{eff} is put in the above equation we get finally an interesting result

$$\delta_{3dB} \cong \frac{d}{2}$$

Thus, the above result indicates that the cross-range resolution of the SAFT system is independent of the ultrasonic frequency and range if the effective aperture L_{eff} is used for the shortest wavelength in the ultrasonic signal. The smaller the single transducer is used, the finer resolution can be obtained. It should be noted, however, that the minimal transducer size is limited by the signal to noise ratio required for target detection.

EXPERIMENTS

A series of experiments was performed to verify the performance of the SAFT algorithms in terms of resolution and grain noise suppression. Selected results are presented below, details can be founds in [9, 10].

Stainless Steel Cube in Contact Mode

The test cube #90646 from Ringhals Power Plant made of cast austenitic steel was inspected in contact mode. There are two groups of holes in the cube that were possible to detect.
Three side drilled holes (SDHs) with different diameters at the depth of approximately 40 mm were used as targets. The location of the holes is clearly illustrated in Fig. 4, where the test parameters are also listed.

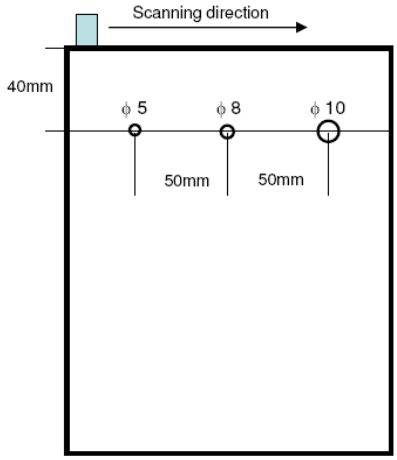

Transducer	Panametrics 2.25 MHz; 0.5 inch
Material Velocity	5800 m/s
Sampling frequency	80 MHz
Scanning step	0.5 mm
Synthetic aperture	36 mm
B-scan -3 dB width SAFT -3dB width *d*/2 Noise level improvement	27.3 mm 5.1 mm 6.35 mm 4 dB

Figure 4 – Location of the three SDHs in the SS cube and ultrasonic parameters of the test.

The original B-scan data and the SAFT result are plotted in Fig. 5. It can be seen that the resolution of the raw B-scan is quite poor (27.3 mm) and a high level of material noise is observed. After SAFT processing, the resolution is improved to approx. 5 mm and the noise level is reduced. The resolution of SAFT is approximately half of the transducer diameter, as discussed previously. Note, that the holes have relatively large diameter, which has an apparent effect on the time of flight at the B-scan responses and the SAFT results. The response to the largest hole (the right one) appears at the shorter range than that of the smallest one.

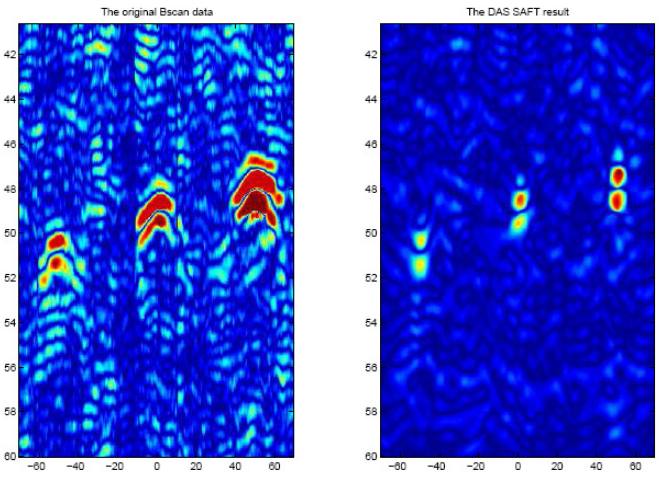

Figure 5 – B-scans of the 3 holes in the SS cube in contact mode. Raw data (left) and the result of SAFT processing (right).

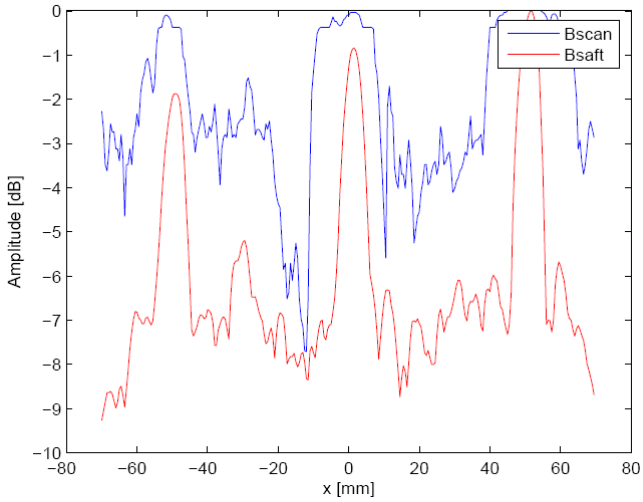

Figure 6 – Cross-range profiles for the SS cube.

To compare resolution and noise level at B-scans cross-range profiles were calculated by plotting maximum amplitudes in each A-scan as a function of transducer position on *u* axis (see Fig. 1). From the profiles presented in Fig. 6 it can be seen that the structure noise level after SAFT processing has been decreased with approx. 4 dB comparing with that in the raw B-scan data.

Copper Block in Immersion Mode

A copper test block with coarse structure was inspected in immersion. This block had a number of SHDs with diam. 1 mm drilled at different depths from the upper surface. The SDHs located at the depths 20 mm, 24 mm, 28 mm and 32 mm were detected in the test. Due to the material structure a transducer with relatively low center frequency (2.25 MHz) was chosen for this test. The results of this test are shown in Fig. 7. Cross-range profiles are shown in Fig. 8 where the test parameters are also listed.

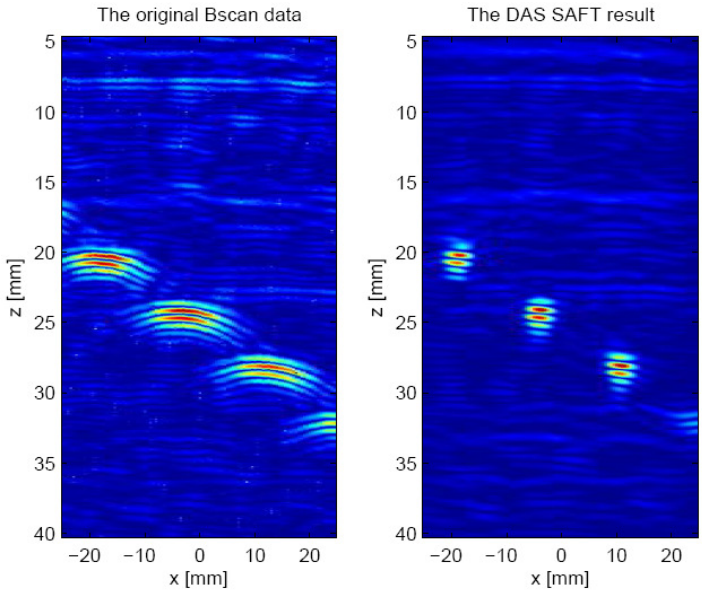

Figure 7 – B-scans of the 4 holes in the copper block in immersion mode. Raw data (left) and the result of SAFT processing (right).

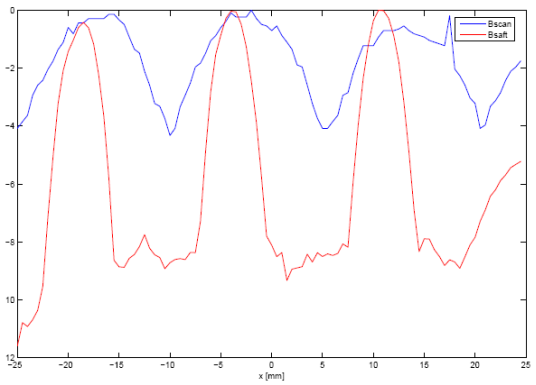

Transducer	Panametrics 2.25 MHz; 0.375 inch
Material Velocity	4660 m/s
Sampling frequency	80 MHz
Scanning step	0.5 mm
Water path	64 mm
Synthetic aperture	36 mm
B-scan -3 dB width SAFT -3dB width *d*/2	38 mm 3.3 mm 5 mm

Figure 8 – Cross-range profiles for the SS cube and the list of the immersion test parameters. The B-scan and SAFT -3dB widths were respectively, 38 mm and 3.3 mm.

In summary, the performed tests show that the t-d SAFT is capable of improving both the cross-range resolution and suppressing the grain noise. The noise suppression is well pronounced but not such impressive as the resolution improvement. It is expected that the frequency domain SAFT, presented recently in [3] will be more effective in this respect.

CONCLUDING REMARKS

SAFT algorithms for post-processing ultrasonic data acquired in ultrasonic inspection of coarse structured metals were investigated in this report. SAFT algorithms for contact and immersion inspection were considered and their performance was investigated using real ultrasonic RF signals.

The experimental results presented in this report indicate that the time-domain SAFT algorithms yield considerably improved cross-range (lateral) resolution comparing with the original B-scans for a wide range of target depths for materials with coarse structure. The improved resolution was always better than the theoretical limit for SAFT, equal to half transducer diameter.

As expected, SAFT processing also yields an improved ratio of the ultrasonic defect response to the structure noise level. The observed improvement was in the range of 3 to 5 dB depending on the setup and the test frequency. It is expected that this improvement could be even better if the more efficient frequency-domain SAFT was applied.

It should be pointed out that the classical SAFT schemes considered in this report can be seen as the 2D spatio-temporal filters while the acoustic lens performs the 3D processing of the ultrasonic data. Although extension of the 2D SAFT with third dimension does not present any theoretical problems it is still difficult due to the practical limitations of the today's NDE systems as well as the storage and computing resources required for this purpose. The viable solution, already tested by some system manufacturers, seems to be providing the phased array systems with powerful processing resources in real-time to avoid post-processing large data volumes.

The experimental results presented in this preliminary study are positive, that is, SAFT is capable of improving the lateral resolution and suppressing structure noise in ultrasonic inspection of coarse structured materials.

REFERENCES

[1] F. Lingvall, T. Olofsson and T. Stepinski, "Synthetic aperture imaging using sources with finite aperture-deconvolution of the spatial impulse response", *J. Acoust. Soc. Am.*, 2003, 114 (1), 225-34.

[2] F. Lingvall, *Time domain reconstruction methods for ultrasonic array imaging*, PhD thesis, Uppsala University, Signals and Systems, 2004.

[3] T. Stepinski, “An implementation of synthetic aperture focusing technique in frequency domain”, *IEEE Trans. on Ultrasonics, Ferroelectrics, and Frequency Control*, 2007, 54(7), 1399-1408.
[4] J.A. Seydel, *Ultrasonic Synthetic-aperture Focusing Techniques in NDT*, Research Tech- niques for Nondestructive Testing, Academic Press, 1982.
[5] V. Schmitz, S. Chalkov, and W. Muller, “Experience with synthetic aperture focusing tech- nique in the field”, *Ultrasonics*, 2000, 38, 731-38.
[6] S.R. Doctor, T.E. Hall, and L.D. Reid, “SAFT – the evolution of a signal processing technology for ultrasonic testing”, *NDT International*, 1986, 38, 165-67.
[7] M. Soumekh, *Synthetic aperture radar signal processing*, John Wiley & Sons Ltd., 1999.
[8] L.J. Cutrona, “Comparison of sonar system performance achievable using synthetic-aperture technique with the performance achievable by more conventional means”, *J. Acoust. Soc. Am.*, 1975, 58(2), 336-348.
[9] Kefei Lu, “Synthetic aperture focusing technique in immersion mode ultrasonic imaging” Master thesis, Chalmers University of Technology, 2007.
[10] Jing Liu, “Synthetic aperture focusing technique in ultrasonic imaging”, Master thesis, Chalmers University of Technology, 2007.